J Appl Electrochem (2009) 39:2461–2467
DOI 10.1007/s10800-009-9937-8

ORIGINAL PAPER

Ionic liquids based on 1-aza-bicyclo[2,2,2]octane (Quinuclidine) salts: synthesis and physicochemical properties

Jean-Yves Kazock · Mohamed Taggougui · Meriem Anouti · Patrick Willman · Bernard Carré · Daniel Lemordant

Received: 31 January 2008 / Accepted: 29 May 2009 / Published online: 14 June 2009
© Springer Science+Business Media B.V. 2009

Abstract A series of new hydrophobic ionic liquids based on 1-alkyl-quinuclidinium cations, quoted as C_nQuin^+ where n is the number of carbon atoms in the alkyl chain, and on the fluorinated anion bis(trifluoromethanesulfonyl)imide ($TFSI^-$) were synthesized, characterized by NMR (^1H, ^{13}C), and their elemental analysis determined. Among the five compounds synthesized, only one: $C_6Quin(TFSI)$ is liquid at ambient temperature and the others with the exception of $C_1Quin(TFSI)$, exhibit melting points below 100 °C and can be considered as ionic liquids. With the aim of using them as electrolytes in electrochemical devices, some of their physicochemical properties such as density, dynamic viscosity and conductivity were explored. The behaviour of $C_6Quin(TFSI)$ at a graphite electrode was investigated in the presence of added LiTFSI, by means of cyclic voltammetry for possible use as electrolyte in Li-ion batteries. Results show that the large quinuclidinium cations intercalate in the graphite layers and do not permit the reversible insertion of lithium ions.

Keywords Quinuclidine · *N*-quaternary ammonium salts · Lithium ion · Ionic liquids · Batteries

J.-Y. Kazock (✉) · M. Taggougui · M. Anouti · B. Carré · D. Lemordant
Faculté des Sciences et Techniques, Physicochimie des Matériaux et des Biomolécules (EA 4244), Université de Tours, Parc Grandmont Bat. J, 37200 Tours, France
e-mail: jykazock@yahoo.fr

P. Willman
CNES, 18 Avenue E. Belin, 31055 Toulouse cedex, France

1 Introduction

Since the discovery of the first ionic liquid, ethyl ammonium nitrate ($[EtNH_3^+][NO_3^-]$), reported as early as 1914 by Walden [1], there has been, in recent years, a growing scientific and commercial interest in the synthesis and application of ionic liquids (ILs). This increasing interest is illustrated by the exponential increase in the number of papers concerning ILs over the past 10 years [2–8].

Ionic liquids may be defined as salts which have at least one organic cation and one inorganic anion and which are liquids at temperatures below 100 °C [9–11]. They possess a number of useful properties: negligible vapor pressure, excellent thermal stabilities, polar and non-coordinating properties, solvating properties toward organic molecules or ionic compounds and so on. ILs are of interest in several fields of research including catalysis, electrochemistry, chemical engineering and more generally contribute to the development of what is called "green" chemistry because their utilization will greatly reduce environmental risk [12–15]. In biology, some ILs have been reported to demonstrated anti-microbial activities against bacteria and fungi and biodegradability properties [16–19].

One key area of research is the use of IL-based electrolytes for lithium ion rechargeable batteries, capacitors, solar cells and other electrochemical devices [20, 21]. Improving the performance of electrochemical systems in term of security is a goal that has prompted us to search for new ionic liquids. Most ILs described to date are, to the best of our knowledge, combinations of charge delocalized inorganic anion and cations like 1-alkyl-3-methylimidazolium, *N*-alkylpyridinium, pyrrolidinium, pyrimidinium or tetraalkylpyrrolidinium [20]. Compared with the imidazolium system, aliphatic quaternary ammonium (AQA) ions are desirable as IL's cationic part as they are electrochemically

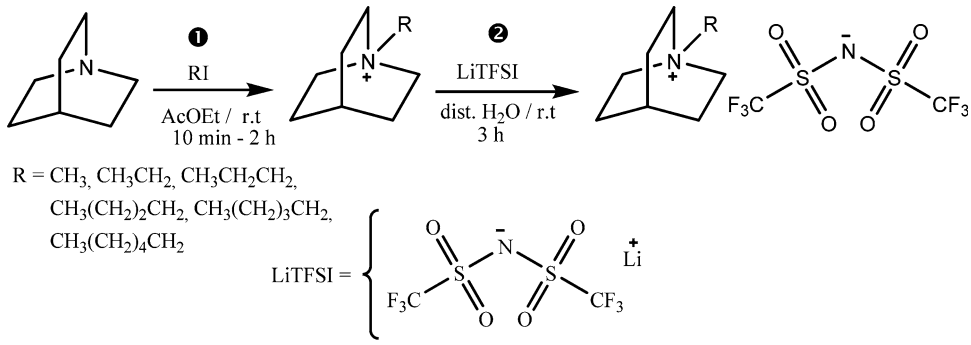

Fig. 1 C_nQuin(TFSI) synthesis procedure (*n* indicates the number of carbon)

and thermally stable against oxidation and reduction. Nevertheless, in order to obtain a liquid phase at ambient temperature, AQA have to associate with large organic fluorinated anions. The bis(trifluoromethanesulfonyl)imide (TFSI) is one of the best candidates for this purpose as this fluorinated anion is also thermally stable and, associated with AQA, forms electrochemically stable ionic liquids. Moreover, the TFSI anion leads to ionic liquids which have substantially lower melting points and higher fluidity than almost any other anions [22]. The organic salts of the TFSI anion are also generally hydrophobic.

We report here for the first time the preparation of ionic liquids based on the polycyclic amine azabicyclo [2,2,2]octane after alkylation as a quaternary alkylammonium cation (quinuclidinium) and the bis(trifluoromethanesulfonyl)imide (TFSI). This new series of ILs, quoted as C_nQuin(TFSI) where *n* is the number of carbons in the alkyl chain, was prepared accorded to the scheme shown in Fig. 1 and characterized by NMR spectra and elemental analysis. The synthesis of a series of similar compounds, based on 1,4-diaza-bicyclo[2,2,2]octane (dabco), has already been reported [23] but these ILs present a Lewis base site on the cation which gives them different chemical properties. Moreover, the presence of a free electron pair on the nitrogen atom of the dabco derivatives is not desirable for the present electrochemical application.

In this work, some of physical properties of these ILs are reported such as density, viscosity, conductivity and electrochemical window.

2 Experimental section

2.1 Materials

Unless otherwise noted, all reagents were purchased from Sigma-Aldrich, Alfa Aesar with the exception of LiTFSI, which was provided by Solvionic (Toulouse, France) and used without further purification. A Metrohm Karl Fisher Coulometer 831 was used to determine the water content of the samples.

NMR spectra were run at 200 MHz (^{1}H) and 50 MHz (^{13}C) in DMSO-d_6 or $CDCl_3$ on a Bruker-DPX-200 instrument and chemical shifts (δ) are reported in parts per millions (ppm).

Differential Scanning Calorimetry (DSC) was performed on a Perkin–Elmer DSC-6 apparatus. Samples were placed in aluminum pans, which were sealed in a dry box. Scans were performed at 10 °C min^{-1} (heating) from 25 to 400 °C.

ILs densities were determined by weighing samples contained in 5 mL pycnometer for which the stopper was equipped with a fine capillary. Each measurement was repeated three times and only the average value is reported.

Dynamic viscosities were measured by a rotational rheometer (AR 1000, TA Instruments) with an estimated error of ±0.1%; rheogramms were obtained using a standard steel cone geometry (diameter, 60.0 mm; angle, 00°29′3″) at temperatures ranging from −5 to 90 °C. As these liquids are Newtonian, a constant shear rate of 40 rad s^{-1} was applied for all samples.

ILs conductivities were measured by means of the complex impedance method with the aid of a Solartron SI 1260 Impedance analyser and a 1287 electrochemical interface coupled to a computer over a frequency range from 1 to 10^6 Hz. An AC perturbation of 10 mV was applied to the cell (having a constant of 0.109 cm^{-1}). The real and imaginary parts of the complex impedance were plotted, and the ionic conductivity was deduced from the bulk resistance determined at the intercept with the real axis of the first loop on the impedance diagram.

Graphite electrodes were a gift from SAFT (Bordeaux, France). Graphite/Li half-cells were built using Swagelock® connectors and cycled with an Arbin battery cycler. Cyclic voltammograms were obtained at a 0.1 mV s^{-1} scan rate between 0 and 3 V versus Li/Li$^+$.

2.2 Synthesis

According to the reaction scheme presented in Fig. 1, the synthesis of 1-alkyl-quinuclidinium bis(trifluoromethanesulfonyl)imide [C_nQuin(TFSI)] was accomplished by

metathesis anion-exchange between bis(trifluoromethanesulfonyl)imide lithium salt and the 1-alkyl-quinuclidinium iodide in distilled water at room temperature. All details concerning the synthesis and the characterization of the compounds are presented in the appendix.

As reported previously [24], 1-alkyl-quinuclidinium iodides were prepared in a one step procedure. *N*-quaternary ammonium iodides were used as starting materials to obtain [C_nQuin(TFSI)] ILs. To ensure a maximum of purity, synthesized ILs were washed repeatedly in distilled water and the halide-free was monitored qualitatively by a silver nitrate test [25]. ILs were dried under vacuum at 90 °C for 48 h and stored in a dry box after drying. Their purity was established by clean acquisition of ^{1}H and ^{13}C NMR (see data in appendix) and their water content, generally below 80 ppm, was determined by Karl-Fischer titration.

3 Results and discussion

3.1 Synthesis results and DSC measurements

As seen in Table 1, which summarizes synthesis results as well as some physicochemical properties, all compounds were efficiently synthesized, the yield ranging from 75% to 93%. Even though all ILs have a hydrophobic character as they do not mix with water, they are still hygroscopic, but this property is common to many ILs [26].

As an example, the thermogramm of C_1Quin(TFSI) (**1**) is reported in Fig. 2. This compound displays a melting point at 139 °C and a solid-solid phase transition at 67 °C but it is the sole compound of this series which exhibits a solid–solid phase transition. As the freezing point is lower than the melting point, it can be concluded that substantial supercooling occurs. C_1Quin(TFSI) exhibits a wide thermal stability as no vaporization occurs below 280 °C. Between 280 and 400 °C, a large endothermic peak is observed which corresponds to the vaporization of the IL, but without any decomposition as, on the following cooling sweep, the freezing enthalpy (−27.4 kJ mol^{-1}) is practically the opposite of the melting enthalpy (25.3 kJ mol^{-1}).

Other 1-alkyl-quinuclidinium TFSI present similar thermogramms and, as seen in Table 1, the melting points (mp) of these salts decreases when increasing alkyl chain length. We also observed substantial supercooling as the freezing points (T_{freez}) of the samples are lower than their melting points by about 30 °C for compounds (**1**) and 10 °C for (**2**), (**3**) and (**4**).

With the exception of compound (**1**), all ILs have a melting point below 100 °C but only compound C_6Quin(TFSI) (**5**) melts at room temperature. Melting points of alkylquinuclidinium TFSI are lower than their corresponding iodide salts as reported previously [24]. Compound (**5**) which is liquid at ambient temperature is the unique real room temperature ionic liquid (RTIL) and, for this reason, its physicochemical and electrochemical properties have been investigated in detail. This compound also exhibits the supercooling phenomenon as it remains liquid even at 0 °C.

3.2 Density of C_6Quin(TFSI)

Data obtained from density measurements are reported in Table 1 for solid ILS (**1–4**) and for the RTIL (**5**). Compounds (**1**), (**2**) and (**3**) exhibit low densities (<1.12 g cm^{-3}) at 25 °C in contrast with compound (**4**) and (**5**) for which the density is over 1.35 g cm^{-3}. This means that high molecular weight C_nQuin(TFSI) have a more compact structure than their lighter homologues.

For the RTIL, compound (**5**), the density was measured as a function of the temperature as reported in Fig. 3. Density variations (d) with the temperature (θ), expressed in °C, follows a linear relation:

$$d = d^{\circ} + a\theta \quad (1)$$

In Eq. 1, d°(density at 0 °C) = 1.372 g cm^{-3} and a = 8.25 × 10^{-4} g cm^{-3} K^{-1}. The density of C_6Quin(TFSI) at 25 °C is 1.352 g cm^{-3}.

3.3 Dynamic viscosity

In contrast to the melting points, which decrease with the alkyl chain length, viscosities increase from 12.41 mPa s

Table 1 Synthesis yield and properties of 1-alkyl-quinuclidinium imide salts at 25 °C

Compound	Molecular weight (g mol)	Yield/%	T_{s-s}/°C (±2 °C)	T_{free}°C (Undercooling)	mp/°C (±2 °C)	η/mPa s (±5%)	Density/g cm^{-3} (±0.002)
1 C_1Quin(TFSI)	406.37	81	67	111	139	–	1.046 (solid)
2 C_2Quin(TFSI)	420.39	80	–	59	79	12.41[b]	1.024 (solid)
3 C_3Quin(TFSI)	434.42	81	–	64	70	20.11[c]	1.113 (solid)
4 C_4Quin(TFSI)	448.45	75	–	38	51	26.28[b]	1.419 (solid)
5 C_6Quin(TFSI)	476.50	93	–	–	13.7[a] (± 0.5)	413.30[d] 40.88[e]	1.352 (solid)

[a] obtained by heating from −16 °C to r.t; [b]88 °C; [c]88.9 °C; [d]25.1 °C; [e]79.9 °C

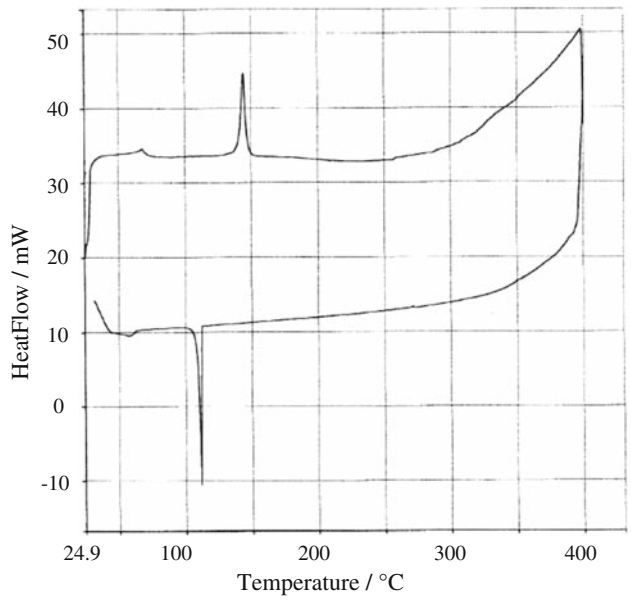

Fig. 2 DSC thermogramm for C_1Quin(TFSI) at rate of 10 °C min^{-1}

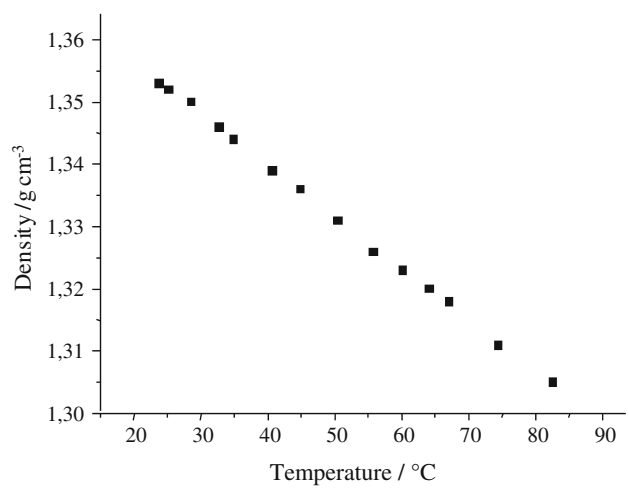

Fig. 3 Density of C_6Quin(TFSI) versus temperature

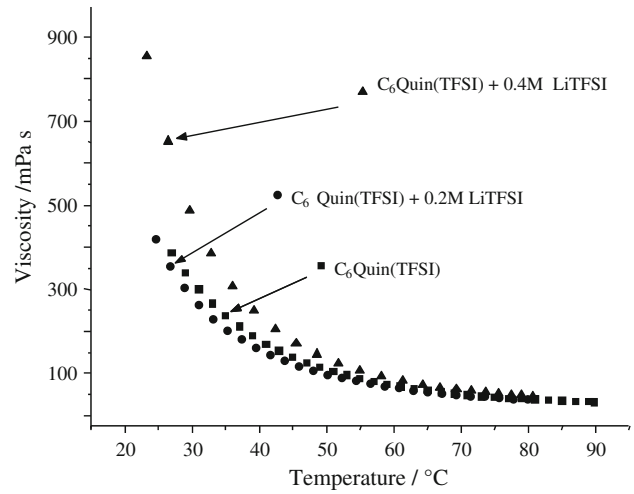

Fig. 4 Dynamic viscosities of C_6Quin(TFSI) (*filled square*) and two of its mixture with LiTFSI 0.2 M (*filled circle*) and 0.4 M (*filled triangle*)as a function of the temperature

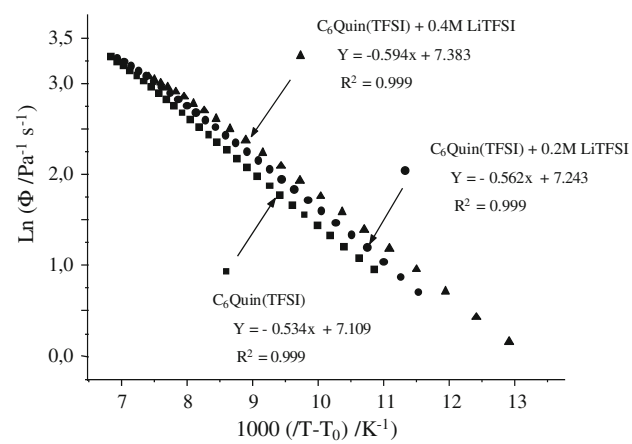

Fig. 5 VTF plot of the fluidity for C_6Quin(TFSI) and mixtures with LiTFSI

(at 88 °C) for compound (**2**) to 40.88 mPa s (at 79.9 °C) for compound (**5**) as reported in Table 1.

The viscosity of the RTIL C_6Quin(TFSI) (**5**) was investigated as a function of the temperature in the range −5 to 80 °C. In addition, some liquid mixtures containing different concentrations of LiTFSI were also investigated as possible electrolytes for Li-ion batteries. The viscosity variations of pure C_6Quin(TFSI) and mixtures with LiTFSI are reported in Fig. 4. The dynamic viscosity of the three solutions is highly temperature dependent. The viscosity of C_6Quin(TFSI) which is equal to 474 mPa s at room temperature is reduced to 50.1 mPa s at 70 °C.

Under the addition of LiTFSI, no significant variations occur when the concentration is 0.2 M, but when the concentration is increased to 0.4 M, a sharp increase in viscosity is observed: from 62 mPa s (pure RTIL at 69.3 °C) to 853 mPa s in the presence of 0.4 M LiTFSI. Thus, according to this result, the addition of small lithium ions to the RTIL induces strong electrostatic interactions between ions of opposite charge as previously noted [27, 28]. Nevertheless, it is surprising that at a concentration of 0.2 M or below, no effect occurs.

As seen in Fig. 5, the variations of Ln(Φ) versus $1/(T - T^0)$, where Φ ($=\eta^{-1}$) represents the fluidity and $T°$ is a fitting parameter which corresponds to the ideal glass transition temperature, are represented by straight lines for C_6Quin(TFSI) and its mixtures with LiTFSI. The linearity of the graphs indicates that the viscosities verify the VTF theory [29] and the corresponding values of T^0 are reported in Table 2.

Table 2 T^0 and their corresponding °C values of compound **5** and mixtures with various amounts of LiTFSI

Solutions	T^0/K	T/ °C
C_6Quin(TFSI)	209	−65.15
C_6Quin(TFSI) + 0.2 M LiTFSI	209	−65.15
C_6Quin(TFSI) + 0.4 M LiTFSI	219	−54.15

3.4 Conductivity

Arrhenius plots of the ionic conductivity of C_6Quin(TFSI) and two of its mixtures with LiTFSI are shown in Fig. 6. The conductivity of this RTIL at ambient temperature (25 °C) is 0.36 mS cm^{-1}. This value can be compared to that found for *n*-hexyl-trimethylammonium imide: 0.67 mS cm^{-1} [30, 31]. This shows that the rigid cycle structure of the quinuclidinium cation leads to less conductive and more viscous solutions (413.3 mPa s and 167 mPa s, respectively, for C_6Quin(TFSI) and *n*-hexyl-trimethylammonium(TFSI)). These two cations are not very different in size as their van der Waals volume are 0.137 nm^3 for the bicyclic cation and 0.110 nm^3 for the acyclic *n*-hexyl-trimethylammonium cation. This means that it is the size of the head group which is largely responsible for the difference in mobility.

As seen in Fig. 6 the addition of LiTFSI to the RTIL decreases the intrinsic conductivity of the RTIL from 0.36 to 0.24 and 0.16 mS cm^{-1}, respectively, for 0.2 M and 0.4 M in LiTFSI. The ionic conductivity (σ) of all solutions depends largely on temperature but does not follow the simple Arrhenius law as the corresponding Ln(σ) versus 10^3/T plot is not linear in the range of temperatures investigated. A better fit to the experimental results is obtained by plotting the variation of Ln(σ) with $10^3/(T - T^0)$ according to the VTF equation (2) [29]:

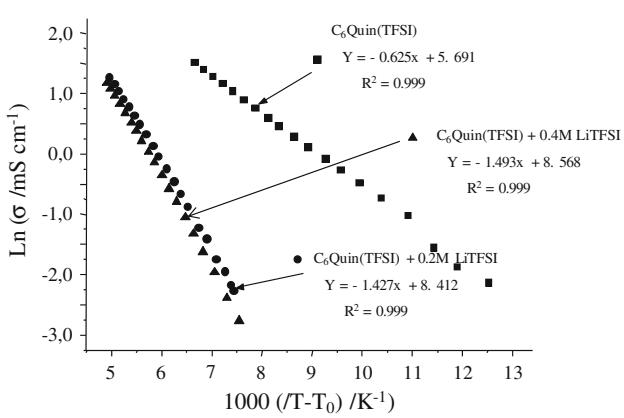

Fig. 6 Conductivity variations of C_6Quin(TFSI) (*filled circle*); C_6Quin(TFSI) + 0.2 M LiTFSI (*filled triangle*) and C_6Quin(TFSI) + 0.4 M LiTFSI (*filled square*) with the temperature

Table 3 Parameters of the VTF (Eq. 2 in the text): *A* and *T*° the ideal glass transition temperature for compound (**5**). The accuracy of the fitting procedure is given by the regression coefficient R^2

Parameter	*A*/kJ mol^{-1}	*T*°/K	R^2
C_6Quin(TFSI)	4.4	204	0.998
C_6Quin(TFSI) + 0.2 M LiTFSI	4.6	151	0.999
C_6Quin(TFSI) + 0.4 M LiTFSI	4.9	151	0.999

$$\sigma = \sigma^\circ \exp(-A/R(T - T^\circ)) \quad (2)$$

In Eq. 2, A is a fitting parameter which is linked to configurational entropy and T° is the ideal glass transition temperature, i.e. the temperature at which the viscous liquid is transformed to a glassy solid. The T° values for the RTIL and its mixtures with LiTFSI are reported in Table 3, and it appears that the mixtures exhibit the same glass transition temperature.

3.5 Cyclic voltammetry

In order to test synthesized RTIL as electrolyte for lithium-ion batteries, LiTFSI was added to the C_6Quin(TFSI) RTIL. As in Li-ion batteries, the negative graphite electrode is very sensitive to the electrolyte composition and, particularly, cannot work properly without the formation of a passive layer, the first tests were operated using the following half cell:

Li/C_6Quin(TFSI) + LiTFSI/graphite.

Figure 7 shows the successive cyclic voltammograms obtained using C_6Quin(TFSI) as electrolyte in the graphite half-cell. A first small cathodic peak $E_{pc,1} = 1.66$ V vs. Li/Li^+ is observed at the first cathodic sweep. This peak is attributed to the reduction of residual water. The second peak at $E_{pc,2} = 0.8$ V, which appears only at the first cathodic scan, corresponds to the formation of the solid electrolyte interface (SEI) on the graphite surface as it is not visible at the second cycle. The broad cathodic peak $E_{pc,3} = 0.5$ V is attributed to the intercalation of the quinuclidinium cations into the graphene layers [32, 33]. On the reverse scan, an oxidation peak is observed at $E_{pa,1} = 1$ V which corresponds well to the de-intercalation of the quinuclidinium cations. The area under the oxidation peaks at $E_{pa,1}$ increases progressively during the scans, which means that the quinuclidinium intercalation–deintercalation process is increasingly effective.

Figure 8 shows the successive cyclic voltammograms obtained using the mixture C_6Quin(TFSI) + 0.2 M LiTFSI as electrolyte in the graphite half-cell. The peaks at $E_{pc,1} = 1.50$ V and $E_{pc,2} = 0.65$ V are due to the reduction of residual water and to the formation of the passive layer and are not present at the second cycle. The third peak which has a maximum near 0 V is attributed to the

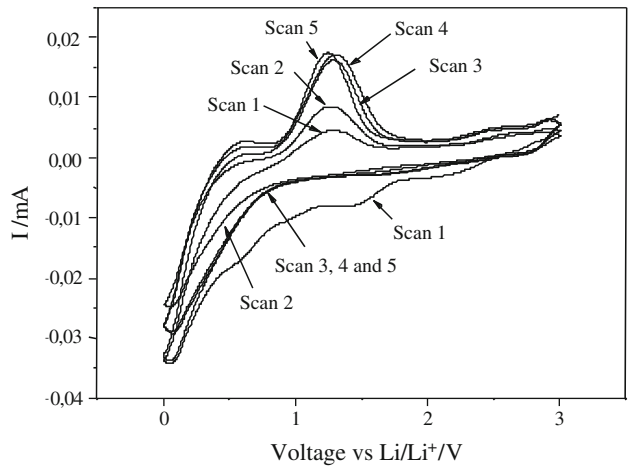

Fig. 7 Cyclic voltamperometry (0.1 mV s^{-1}) of C_6Quin(TFSI) at a graphite electrode

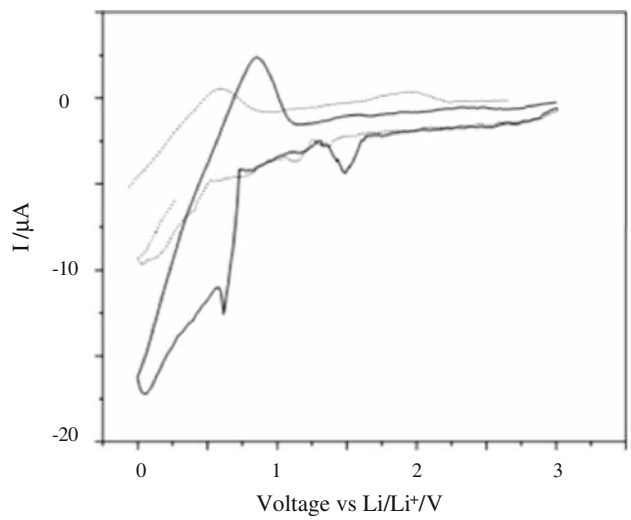

Fig. 8 Cyclic voltamperometry (0.1 mV s^{-1}) of C_6Quin(TFSI) + 0.2 M LiTFSI at a graphite electrode

insertion of quinuclidinium ions as the corresponding anodic peak $E_{pa,1} = 0.8$ V has been identified as the de-insertion potential of these ions. At the second scan only the intercalation and de-intercalation peaks of the quinuclidinium cations are visible. As a result, it is clear that the intercalation of lithium ions is strongly prevented by the co-intercalation of the quinuclidinium cations [34]. Moreover, the quality of the passive layer formed at 0.65 V is questionable, as it is permeable to large quinuclidinium ions which intercalate and possibly lead to the exfoliation of the graphite layers.

4 Conclusions

A new family of hydrophobic organic salts based on the 1-alkyl-quinuclidinium cations and the bis(trifluoromethanesulfonyl) imide as anion have been synthesized and studied. All compounds are ionic liquids (mp < 100 °C) at the exception of C_1Quin(TFSI) which is liquid at 139 °C. The larger molecular weight compound C_6Quin(TFSI) is what is called a RTIL as its melting point is 13.7 °C. Viscosity measurements show that they are viscous liquids and that this parameter increases with the alkyl chain length of the quaternary bicyclo ammonium cation. The conductivity of C_6Quin(TFSI), the sole real RTIL, appears as lower than equivalent quaternary *n*-alkylammonium ions owing to the rigidity and van der Waals volume of the ammonium head. Addition of a lithium salt, like LITFSI, decreases the conductivity of the electrolyte as the small lithium ions reinforce the electrostatic interactions. Cyclic voltammetry show that these compounds cannot be used as electrolyte in Li-ion batteries using graphite as an active material. Future work will be devoted to test other types of cathodic and anodic active material commonly used in Li-ion batteries or as supercapacitors.

Acknowledgments This project was supported by the Centre National d'Etudes Spatiales Toulouse, France under grant no 02/CNES/0750/00 and we express our grateful acknowledgement to Frederic Montigny (SAVIT) for NMR data.

Appendix

Synthetic and characterization details

1-methyl-1-quinuclidinium bis(trifluoromethylsulfonyl) imide (C_1Quin(TFSI)) ***1***: *A* solution of 1-methyl-aza-bicyclo[2,2,2]octane hydroiodide (3.0 g, 11.85 mmol) in distilled water (30 mL) was prepared at r.t. Equimolar amount of bis(trifluoromethanesulfonyl)imide lithium also prepared in distilled water at r.t., was added dropwise into the solution and then the mixture stirred at room temperature for 3 h. The formed precipitate was filtered, washed repeatedly with distilled water to removed any inorganic salt (monitored by a silver nitrate test) and dried in vacuum under reduce pressure at 80 °C to give compound **(1)** as white crystals with good yield. (3.90 g, 81%). mp 139 °C. ^{1}H NMR (δ): 3.40 (t, $J = 7.3$ Hz, 6H, $3CH_2$), 2.90 (s, 6H, $3CH_2$), 2.08 (m, H, CH), 1.88 (m, 6H, $3CH_2$). ^{13}C NMR (δ): 120.35 ($J = 320$ Hz, 2C, $2CF_3$), 56.70 (3C, $3CH_2$), 52.10 (C, CH_3), 24.24 (3C, $3CH_2$), 19.49 (C, CH). Anal. Calcd for $C_{10}H_{16}F_6N_2O_4S_2$: C, 29.56; H, 3.97; N, 6.89%. Found C 29.76, H 3.94; N 6.86%.

1-ethyl-1-quinuclidinium bis(trifluoromethylsulfonyl) imide (C_2Quin(TFSI)) ***2***: Same procedures were applied starting from 3.0 g (11.23 mmol) of 1-ethyl-aza-bicyclo [2,2,2]octane hydroiodide. White crystals (60%). mp 79 °C. ^{1}H NMR (δ): 3.36 (t, $J = 7.4$ Hz, 6H, $3CH_2$), 3.19 (q, 2H, CH_2), 2.08 (m, H, CH), 1.87 (m, 6H, $3CH_2$), 1.22

(t, $J = 7.2$ Hz, 3H, CH_3). ^{13}C NMR (δ): 121.95 ($J = 319.5$ Hz, 2C, CF_3), 59.39 (C, CH_2), 53.98 (3C, $3CH_2$), 24.09 (3C, $3CH_2$), 19.83 (C, CH), 8.10 (C, CH_3). Anal. Calcd for $C_{11}H_{18}F_6N_2O_4S_2$: C, 31.43; H, 4.32; N, 6.66%. Found C 31.36; H 4.38; N 6.75%.

1-propyl-1-quinuclidinium bis(trifluoromethylsulfonyl) imide (C_3Quin(TFSI)) ***3***: Same procedures were applied starting from 3.0 g (10.67 mmol) of 1-propyl-aza-bicyclo[2,2,2]octane hydroiodide. White crystals (3.74 g, 81%). mp 70 °C. ^1H NMR (δ): 3.36 (t, $J = 7.3$ Hz, 6H, $3CH_2$), 3.05 (t, $J = 7.2$ Hz, 2H, CH_2), 2.06 (m, H, CH), 1.87 (m, 6H, $3CH_2$), 1.66 (m, 2H, CH_2), 0.90 (t, $J = 7.3$ Hz, 3H, CH_3). ^{13}C NMR (δ): 120.36 ($J = 320.5$ Hz, 2C, $2CF_3$), 65.54 (C, CH_2), 54.55 (3C, $3CH_2$), 24.13 (3C, $3CH_2$), 19.82 (C, CH), 15.77 (C, CH_2), 11.37 (C, CH_3). Anal. Calcd for $C_{12}H_{20}F_6N_2O_4S_2$: C, 33.18; H, 4.64; N, 6.45%. Found C 33.16; H 4.65; N 6.43%.

1-butyl-1-quinuclidinium bis(trifluoromethylsulfonyl) imide (C_4Quin(TFSI)) ***4***: The same procedures were applied starting from 3.0 g (10.16 mmol) of 1-butyl-aza-bicyclo[2,2,2]octane hydroiodide. White crystals (3.28 g, 72%). mp 51 °C. ^1H NMR (δ): 3.37 (t, $J = 7.9$ Hz, 6H, $3CH_2$), 3.09 (t, $J = 7.1$ Hz, 2H, CH_2), 2.07 (m, H, CH), 1.87 (m, 6H, $3CH_2$), 1.61 (m, 2H, CH_2), 1.30 (m, 2H, CH_2), 0.94 (t, $J = 7.2$ Hz, 3H, CH_3). C ^{13}NMR (δ): 120.36 ($J = 320$ Hz, 2C, $2CF_3$), 63.90 (C, CH_2), 54.51 (3C, $3CH_2$), 24.16 (3C, $3CH_2$), 20.18 (2C, CH_2), 19.85 (C, CH), 14.23 (C, CH_3). Anal. Calcd for $C_{13}H_{22}F_6N_2O_4S_2$: C, 34.82; H, 4.94; N, 6.25%. Found C 34.81; H 4.98; N 6.18%.

1-hexyl-1-quinuclidinium bis(trifluoromethylsulfonyl) imide (C_6Quin(TFSI)) ***5***: The same procedures were applied starting from 3.0 g (9.28 mmol) of 1-hexyl-aza-bicyclo[2,2,2]octane hydroiodide. Liquid transparent (3.6 g, 82%). ^1H NMR: (δ): 3.37 (t, $J = 7.2$ Hz, 6H, $3CH_2$), 3.09(t, $J = 7.2$ Hz, 2H, CH_2), 2.07 (m, H, CH), 1.87 (bs, 6H, $3CH_2$), 1.64 (m, 2H, CH_2), 1.30 (s, 6H, $3CH_2$), 0.91 (t, $J = 7.2$ Hz, 3H, CH_3).C ^{13}NMR (δ) 120.38 ($J = 320$ Hz, 2C, $2CF_3$), 64.11 (C, CH_2), 54.52 (3C, $3CH_2$), 26.41 (CH_2), 24.16 (3C, $3CH_2$), 22.65 (3C, $3CH_2$), 22.10 (C, CH_2), 19.87 (C, CH), 14.51 (C, CH_3). Anal. Calcd for $C_{15}H_{26}F_6N_2O_4S_2$: C, 37.81; H, 5.50; N, 5.88%. Found C 37.74; H 5.59; N 5.84%.

References

1. Walden P (1914) Bull Acad Imper Sci (St Petersburg) 1800
2. Dyson PJ, Grossel MC, Srinivasan N, Vine T, Welton T, Williams DJ, White APJ, Zigras T (1997) J Chem Soc Dalton Trans 3465
3. Dzyuba SV, Bartsch RA (2001) J Heterocycl Chem 38:265
4. Matsumoto H, Kageyama H, Miyzaki Y (2002) Chem Commun 1726
5. Mirzaei YR, Shreeve JM (2003) Synthesis 1:24
6. Handy ST, Okello M, Dickenson G (2003) Org Lett 5:2513
7. Jain N, Kumar A, Chauhan S, Chauhan SMS (2005) Tetrahedron 61:1015
8. Pereiro AB, Tojo E, Rodriguez A, Canosa J, Tojo J (2006) J Chem Thermodyn 38:651
9. Hussey CL (1988) Pure Appl Chem 60:1763
10. Chauvin Y, Olivier-Bourbigou H (1995) Chem Tech 25:26
11. Chauvin Y, Einloft S, Olivier-Bourbigou H (1995) Ind Eng Chem Res 34:2698
12. Freemanfle M (1998) Chem Eng News 76(13):32
13. Andrade CKZ, Takada SCS, Suarez PAZ, Alves MB (2006) Synlett 10:1539
14. Bates ED, Rebecca DM, Ntai I, H Davis Jr (2002) J Am Chem Soc 124:926
15. Gathergood N, Garcia MT, Scammells PJ (2004) Green Chem 6:166
16. Pernak J, Goc I, Mirska I (2004) Green Chem 6:323
17. Gathergood N, Scammells PJ (2002) Aust J Chem 55:557
18. Scammels PJ, Scott JL, Singer RD (2005) Aust J Chem 58:155
19. Cieniecka-Roslonkiewicz A, Pernak J, Kubis-Feder J, Ramani A, Robertsond AJ, Seddon KR (2005) Green Chem 7:855
20. Fernicola A, Scrosati B, Ohno H (2006) Ionics 12:95
21. Wang P, Sakeeruddin MZ, Exnar I, Grätzel M (2002) Chem Commun 24:2972
22. Wykes A, MacNeil SL (2007) Synlett 1:107
23. Yoshizawa-Fujita M, Johansson K, Newman P, MacFarlane DR, Forsyth M (2006) Tetrahedron Lett 47:2755
24. Kazock JY, Taggougui M, Willman P, Carré B, Lemordant D (2007) Synthesis 24:3776
25. Seddon KR, Stark A, Torres MJ (2000) Pure Appl Chem 12:2275
26. Welton T (1999) Chem Rev 99:2071
27. Garcia B, Lavallee S, Perron G, Michot C, Armand M (2004) Electrochim Acta 49:4583
28. Nakagawa H, Izuchi S, Kuwana K, Nukuda T, Aihara Y (2003) J Electrochem Soc 150:A695
29. Angell CA (1964) J Phys Chem 68:1917
30. MacFarlane DR, Sun J, Golding J, Meakin P, Forsyth M (2000) Electrochim Acta 45:1271
31. Sun J, Forsyth M, MacFarlane DR (1998) J Phys Chem B 102:8858
32. Fuller J, Carlin CT, Osteryoung RA (1997) J Electrochem Soc 6:3881
33. Zheng H, Jiang K, Abe T, Ogumi Z (2006) Carbon 44:203
34. Mabuch A, Kokmitsu T, Fujimoto H (1995) J Elelctrochem Soc 142:1041